Immunohistochemical quantification of $5HT_{2C}$ receptors and Ca_V 1.3 channels after spinal cord injury in the upper lumbar mouse spinal cord

Honors Thesis

Presented to the College of Agriculture and Life Sciences,

Biological Sciences of Cornell University

In

Partial Fulfillment of the Requirements for the

Research Honors Program

by

Gabrielle N. Van Patten

May 2011

Dr. Ronald M. Harris-Warrick

Immunohistochemical quantification of $5HT_{2C}$ receptors and Ca_V 1.3 channels after spinal cord injury in the upper lumbar mouse spinal cord

Gabrielle N. Van Patten and Ronald M. Harris-Warrick
Department of Neurobiology and Behavior, Cornell University, Ithaca, NY 14853.

The mammalian hindlimb central pattern generator (CPG) for locomotion is located in the lumbar spinal cord, and coordinates contralateral alternation of the hindlimbs and intralimb flexor/extensor muscle alternations. Serotonin (5HT) plays an important role in enabling CPG functionality. All serotonergic input to the lumbar cord descends from the medullary Raphe nuclei; these inputs are lost after a complete spinal cord lesion. We used immunohistochemical methods to determine whether spinal cord injury (SCI) affects the expression levels of $5HT_{2C}$ receptor clusters and Ca_V 1.3 channel clusters. Quipazine is a $5HT_2$ agonist and its regular administration has previously led to partial locomotor recovery. We sought to determine if daily administration would reduce the SCI-induced homeostatic changes in $5HT_{2C}$ receptor and Ca_V 1.3 channel levels. Half the SCI mice were treated with quipazine, and half were saline vehicle treated. A combination of ImageJ and Matlab was used to determine the number, size, and intensity of $5HT_{2C}$ receptor clusters after SCI, as well as the percentage of the frame area covered by Ca_V 1.3 channels and their average brightness. After SCI, there is a significant upregulation in the number of $5HT_{2C}$ receptor clusters, and $5HT_{2C}$ receptor clusters are significantly larger. Neither is reduced by quipazine. There is no significant change in the average brightness of $5HT_{2C}$ receptor clusters after SCI. Additionally, the area and intensity of Ca_V 1.3 channels are significantly larger in SCI/saline mice than in intact mice. Ca_V 1.3 channels were not examined in SCI/quipazine mice due to a small sample size.

Introduction

All animals exhibit some type of locomotor rhythmicity, such as respiration, chewing, digestion in the gastrointestinal tract, swimming, or walking, which is not controlled consciously. To generate rhythmic locomotor outputs, the central nervous system must have some internal driving rhythm. Typically, rhythmic locomotor outputs are controlled by a central pattern generator (CPG), a network of neurons that can have very complex excitation and inhibition circuits. CPGs can be composed of many types of neurons with different intrinsic properties and sensitivities to various neuromodulators, and the

presence of many types of neurons can generate relatively complex rhythmic locomotor outputs.

The mammalian hindlimb CPG for locomotion is responsible for coordinating left/right alternation of the hind limbs, as well as the flexor/extensor muscle alternations in each limb required to make a step, and these alternations occur in the absence of sensory inputs (Kiehn 2006). The hindlimb locomotor CPG is distributed through the lower thoracic and lumbar segments of the spinal cord, but is primarily concentrated in the upper lumbar region of the spinal cord (Kiehn 2006). This CPG involves a complex network of neurons that can generate rhythmic activity in the absence of sensory inputs, although sensory inputs can alter locomotor output (Kiehn 2006; Harris-Warrick 2010).

The hindlimb CPG receives serotonergic input from descending serotonergic fibers in the Raphe nuclei of the brainstem (Ballion et al. 2002; Jordan et al. 2008). Application of serotonin (5-hydroxytryptamine or 5HT) and NMDA (N-methyl-D-aspartate) to whole cord preparations of the isolated neonatal mouse spinal cord can produce fictive locomotion that possesses the necessary criteria for locomotion: left/right interlimb alternation as well as intralimb flexor/extensor muscle alternation (Zhong et al. 2010). 5HT plays a complex but not fully understood role in generating locomotor outputs (Schmidt and Jordan 2000). 5HT is known to increase motoneuron excitability (McCall and Aghajanian 1979); however, its actions are likely indirect as 5HT only produces a subthreshold depolarization of motoneurons in the absence of glutamate (VanderMaelen and Aghajanian 1980; Jackson and White 1990; White and Neuman 1983). Likely, it plays a modulatory role, “priming” the CPG so that it can respond to

glutamatergic input that activates motoneurons to generate to locomotor output (Schmidt and Jordan 2000).

When the neuromodulatory inputs to hindlimb locomotor CPG neurons are disrupted, homeostatic changes to these neurons can be expected to occur to counter the change in neuromodulator levels. Homeostasis is a general principle of biology; the body responds to changes in its environment by opposing those changes, so that body conditions remain constant. When there is a decrease in concentration of a neurotransmitter within the central nervous system, receptors that normally bind that transmitter will typically increase expression levels to account for its decreased concentration. Theoretically, homeostasis is maintained, as there is less neurotransmitter but more receptors. However, an increase in receptor expression levels is not always desirable, as in the case of spinal cord injury (SCI).

One result of SCI is a partial or complete loss of descending serotonergic projections from the Raphe nuclei to regions of the spinal cord caudal to the injury site (Cormier et al. 2010; Ballion et al. 2002). Thus, as SCI reduces or eliminates, depending on how complete the lesion is, 5HT in regions caudal to the injury site, it can be expected for homeostatic changes to occur in neurons caudal to the injury that have 5HT receptors or channels. Li et al. (2007) found that motoneurons from SCI rats are sensitive to concentrations of 5HT that are subthreshold for motoneurons from non-injured rats. In SCI rats, these small 5HT concentrations led to higher amplitude persistent inward calcium currents in the motoneurons as compared to intact rats. The authors hypothesize that the muscle spasticity that occurs in humans, rats and mice with spinal cord injuries could be partially explained by this hypersensitivity to 5HT and larger inward calcium

current, which leads to more activation of the motoneurons. As there are still small amounts of endogenous 5HT in the body, a small amount caudal to the injury site can activate super-sensitive motoneurons and cause spasticity (Li. et al. 2007). Another homeostatic change at the neural level that can contribute to muscle spasticity is expression of constitutively active 5HT receptors. Murray et al. (2011) found that there are more constitutively active $5HT_{2C}$ receptors in motoneurons after SCI than in motoneurons from non-injured rats. The authors suggest that having more constitutively active $5HT_{2C}$ receptors could contribute to motoneuron over-activation and thus muscle spasticity, as neurons with constitutively active 5HT receptors can be active in the absence of 5HT (Murray et al. 2011)

In our lab, we have found that Chx-10 interneurons, which are hypothesized to play a role in generating left-right alternation in the locomotor CPG and are located ventral to the central canal (Zhong et al. 2010), are hypersensitive to 5HT after SCI (Husch, unpublished data). Chx-10 interneurons from SCI mice typically respond with at least 1-2 Hertz firing with 0.1 μm 5HT, while Chx-10 interneurons from intact mice typically do not respond with 0.1 μm 5HT. With 1 μm 5HT, intact neurons respond weakly (0-1 Hz), while SCI neurons respond strongly (8-9 Hz), and with 10 μm 5HT, intact neurons increase firing (1-2 Hz) while SCI neurons maintain a high firing frequency (8-9 Hz) (see Fig. 12 for sample recordings). In summary, Chx-10 interneurons from SCI mice respond to smaller concentrations of 5HT than interneurons from intact mice; Chx-10 interneurons are more sensitive to 5HT after SCI. This 5HT sensitivity is likely due to a combination of homeostatic changes that occur after SCI.

In addition to electrophysiological experiments, various immunohistochemical experiments have examined the effect of SCI on the expression levels of 5HT receptors and channels that respond to 5HT in regions caudal to the lesion site. Hayashi et al. (2010) found SERT (5HT transporter) expression levels to be significantly decreased caudal to the injury site after both moderate and severe spinal cord contusions. Because SERT is responsible for the reuptake of 5HT following synaptic transmission and is thus found on synaptic boutons, the loss of serotonergic fibers following SCI may lead to degradation of SERT (Hayashi et al. 2010). SERT degradation may also contribute to neural 5HT sensitivity after SCI; if neurons are activated by small amounts of endogenous 5HT, there are no transporters to recycle it, leading to over-activation of neurons that respond to 5HT. Hayashi et al. (2010) also found a significant upregulation in $5HT_{2C}$ receptors in the sub-lesional ventral spinal cord after severe spinal cord contusion. $5HT_{2C}$ receptor upregulation is yet another mechanism for 5HT sensitivity; small concentrations of 5HT can activate neurons with a large upregulation of 5HT receptors.

One goal of spinal cord injury research is to reduce the negative effects, such as muscle spasticity, of the homeostatic changes that occur after SCI. Various combinations of 5HT receptor subtype agonists have been administered to SCI experimental animals in order to determine which combinations of receptor subtype activations are most effective at providing functional recovery. Daily administration of quipazine, a $5HT_2$ agonist, has been shown to induce partial locomotor recovery after SCI in rats (Antri et al. 2002; Ung et al. 2008). SCI mice receiving vehicle administration lose the ability to exhibit hindlimb plantar stepping, meaning they are unable to place the plantar surface of the foot in

contact with the ground. SCI mice receiving quipazine, however, exhibited partial plantar stepping, so that the plantar surface made some contact with the ground (Antri et al. 2002). However, more successful locomotor recovery is possible with a combination of quipazine and 8-hydroxy-(2-di-N-propylamino)-tetralin or 8-OHDPAT; a $5HT_{1A}$ and $5HT_7$ agonist (Antri et al. 2005). Antri et al. (2005) found that with this treatment, locomotor performance did not decline after treatment was stopped, a promising result for treatment of SCI in humans.

My goal was to determine the expression levels of $5HT_{2C}$ receptors and Ca_V 1.3 channels after SCI in mice, using immunohistochemistry to observe the region of the spinal cord ventral to the central canal, where Chx-10 interneurons are located. As our lab has observed 5HT hypersensitivity in these interneurons after SCI using perforated patch electrophysiology, I sought to determine whether there was an upregulation of $5HT_{2C}$ receptors, which could contribute to the 5HT sensitivity. Additionally, I examined Ca_V 1.3 channel expression after SCI, as increased activation of calcium channels has been shown to occur in motoneurons after SCI (Li et al. 2007). Because daily quipazine administration leads to partial locomotor recovery after SCI, I also wanted to determine whether quipazine counters the homeostatic changes in $5HT_{2C}$ receptor expression that occur in response to SCI.

I found that after SCI, both with and without daily quipazine administration, there is a significant upregulation in the number of $5HT_{2C}$ receptor clusters. Additionally, $5HT_{2C}$ receptor clusters are, on average, significantly larger in SCI mice as compared to intact mice. There is no significant difference between the average brightness of $5HT_{2C}$ receptor clusters between intact, SCI/saline or SCI/quipazine mice. After SCI without

quipazine, the area and intensity of Ca_V 1.3 channels are significantly larger than area and intensity in intact mice. Ca_V 1.3 channels were not examined in SCI/quipazine mice due to a small sample size.

Materials and Methods

Spinal cord injury surgery. 21-day old, Chx10/eCFP mice were anesthetized with ketamine/xylazine IP (0.01 mg/g ketamine, 0.005 mg/g xylazine; intraperitoneal). The dorsal side was then shaved and sterilized with 70% ethanol and betadine. 0.5% lidocaine (0.1cc), lactated Ringer's (containing sodium lactate) (0.025 cc/g), and buprenorphine (0.1 mg/g) were administered subcutaneously. Using aseptic techniques, an incision was made dorsally above the thoracic region of the spinal cord, and layers of fat and muscle were separated to expose the vertebral column. Using forceps, a gap was made between the T8 and T9 vertebrae, and scissors were used to completely transect the spinal cord transversally. The muscles and fat were put back in place, and the incision was closed using tissue glue. 0.01 mg ketoprofen was administered IP, and mice were placed in a heated cage for at least 30 minutes for recovery. The entire procedure, from initial ketamine/xylazine administration to recovery, lasted approximately one hour. As a control for spinal cord injury (SCI) surgery, the surgical procedure described above was carried out on mice until the vertebrae were exposed, upon which the incision was closed with tissue glue (referred to as intact mice). Every subsequent day after surgery, half of the SCI mice received once daily quipazine IP (0.025 mg/g; referred to as SCI/quipazine), and half of the SCI mice received once daily saline (vehicle control; referred to as SCI/saline) IP. Additionally, all mice (intact and SCI) received the

analgesics buprenorphine (IP) for two days after surgery and ketoprofen (IP) for six days after surgery. Mice were euthanized for perfusion 28-35 days after surgery.

Perfusion and spinal cord fixation. Four weeks after SCI surgery, the intact and SCI mice were sacrificed for perfusion. Mice were anesthetized with an overdose of ketamine/xylazine (0.03 mg/g ketamine; 0.015 mg/g xylazine), and the perfusion was started once mice were no longer responsive to a foot pinch. Mice were placed, with the ventral surface exposed, under a fume hood. An incision was made into the peritoneal cavity up to the sternum. The ribcage was cut laterally on the left and right sides, and the diaphragm was cut so that the ventral portion of the ribcage could be removed. An incision was made in the right atrium, and a needle attached to a perfusion pump with perfusion buffer running was inserted in the left ventricle. Mice were perfused with perfusion buffer for three minutes, and then 4% paraformaldehyde (PFA) in 0.1 M phosphate buffer for 20 minutes. Mice were then eviscerated, a laminectomy performed, and the spinal cord removed from the vertebrae.

The L1-L2 (upper lumbar) region of the cord was placed in a 4% PFA, 0.1 M phosphate buffer solution for 1.5 hours at 4^{o}C, then transferred to 30% sucrose solution for 12 hours at 4^{o}C.

Immunohistochemistry. A cryostat was used to make 15 µm transverse sections of the L1-L2 region of one intact, one SCI/saline and one SCI/quipazine mouse (depending on which mice survived four weeks after SCI surgery), all of the same age and surgery date, placed on a single slide (see Fig. 1 for typical example of finished slide). The slides used were Thermo Scientifics' SuperFrost Plus positively charged slides; negatively charged tissue can strongly adhere to the slides, which allows for more rigorous washes.

30 µm coronal sections of the lesion site (cervical and thoracic regions) were also made to ensure completeness of the lesion. Slides were stored at -20°C for up to one week before immunohistochemistry.

A

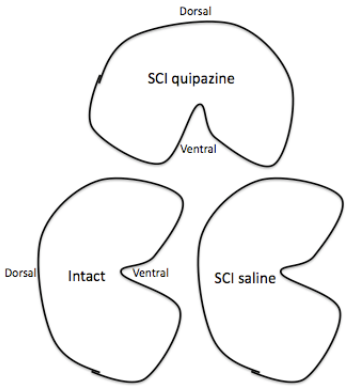

B

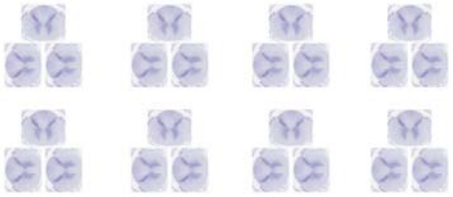

Figure 1. Orientation of tissue on slides. ***A***, one position on a slide. ***B***, entire slide with eight positions. Each position consists of 15 µm transverse sections of the spinal cord, from intact, SCI/saline and/or SCI/quipazine mice, depending on which mice survived four weeks after SCI surgery.

A pap pen was used to enclose each of the eight positions on the slide (see Fig. 1). At room temperature, slides were rinsed in a phosphate buffered saline (PBS) bath for five minutes. Then, slides were incubated in 0.2% Triton X-100 for 10 minutes. Slides were again rinsed with PBS for 15 minutes (for all PBS rinses, 15 minutes = three washes of five minutes each, changing the bath every five minutes). Slices were incubated in peroxidase quenching buffer for 60 minutes at room temperature, and then 1% blocking reagent (source unspecified by manufacturer) for 60 minutes at room temperature. Seven positions were incubated in one primary antibody (5-HT_{2C} 1:200, ABcam; SERT 1:100, Immunostar; 5-HT 1:5000, Sigma; or Ca_V 1.3 1:200, Millipore; all diluted in 1%

blocking reagent), with one position only incubated in 1% blocking reagent (no primary control), for 16 hours at 4^{o}C. Slides were rinsed in 4^{o}C PBS for 15 minutes. Slices were then incubated in secondary antibody conjugated horseradish peroxidase (HRP) diluted 1:100 in 1% blocking solution for 45 minutes at room temperature, and rinsed in PBS for 15 minutes. Slides were then incubated in Alexa-Fluro 647 tyramide, diluted 1:100 in amplification buffer/0.0015% H_2O_2, for 16 minutes. Slides were rinsed in PBS for 15 minutes, mounted with Fluor-Gel and cover-slipped. This tyramide amplification technique is explained in Fig. 2.

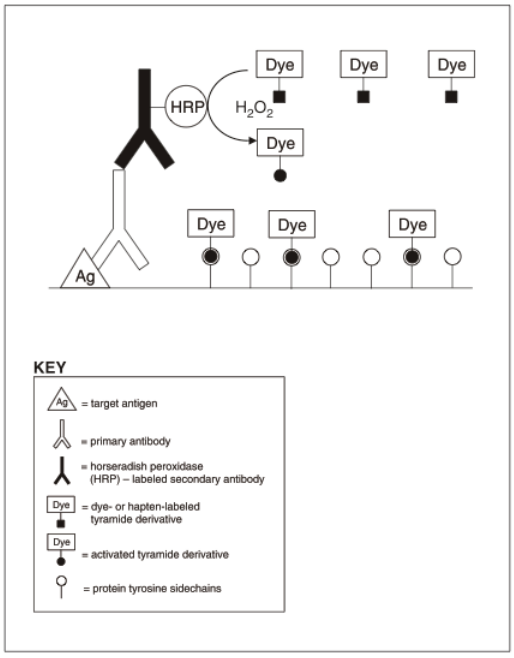

Figure 2. Tyramide amplification mechanism. Unlike conventional immunofluorescence, tyramide immunofluorescence allows for signal amplification. The secondary antibody is conjugated to horseradish peroxidase (HRP), which reacts with an inactive tyramide derivative to produce a fluorescent tag bound to the secondary antibody. This HRP-derivative reaction occurs multiple times at each secondary antibody site, amplifying the signal at each antigen. Tyramide amplification is useful where there is high background noise or few antigen targets. Figure from Invitrogen instruction manual.

Confocal microscopy. A Leica TCS SP2 confocal microscope was used for imaging. A 20-X objective lens was used to view tissue, and boxed regions (8-X zoom) of medial lamina VIII were imaged for analysis (see Fig. 3) using the 633 nm laser line.

Z-series were taken through the 15 µm tissue with the 633 nm laser in one µm steps. ImageJ was used to compile each image stack into a projection with the maximal recorded intensity at each z position displayed in the composite image (max projection).

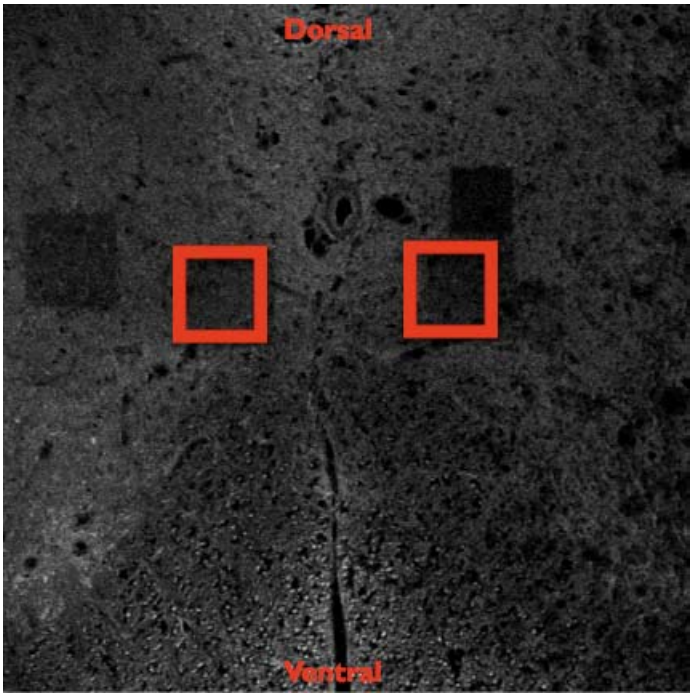

Figure 3. 20-X view of transverse spinal cord section. Red boxes enclose the medial lamina VIII regions of either side of the cord. Both sides of the cord were imaged for analysis at 8-X zoom, for a final zoom value of 160-X.

Image analysis. A combination of ImageJ and Matlab was used for image analysis. For $5HT_{2C}$ immunohistochemistry, intact, SCI/saline and SCI/quipazine images were compared, with n=13 for SCI/saline to intact comparisons, n=5 for SCI/quipazine to intact comparisons, and n=3 for SCI/saline to SCI/quipazine comparisons. The number of receptor clusters, as well as the average size and intensity of receptor clusters per image was compared in the above three combinations of intact, SCI/saline and SCI/quipazine. For $Ca_V1.3$ immunohistochemistry, intact and SCI/saline images were compared (n=4 experiments). SCI/quipazine was not included because there was only one case where the Ca_V 1.3 labeling was successful for SCI/quipazine mice. The percentage of the image

covered by calcium channels and the mean intensity of this area were compared for intact and SCI/saline mice. No analysis was done for SERT labeling, because of a small sample size (n=2 experiments). The details of the analysis steps are outlined in the results section, so as to more clearly depict the results of these analyses.

Results

Loss of serotonergic fibers after spinal cord injury

After spinal cord injury, there is an almost complete loss of serotonergic fibers as compared to intact mice (Fig. 4).

A. Intact, original confocal image

B. SCI, original confocal image

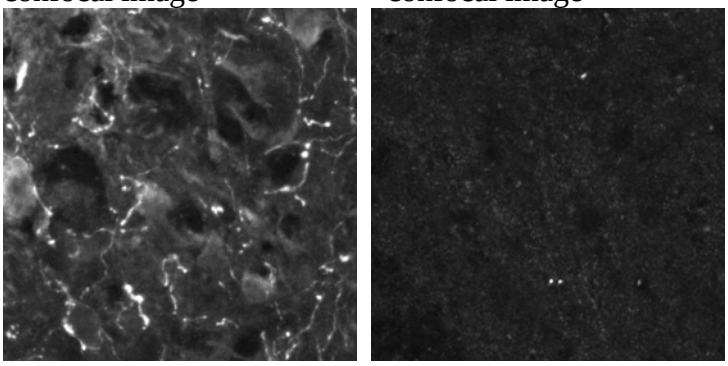

C. Intact, no primary antibody

D. SCI, no primary antibody

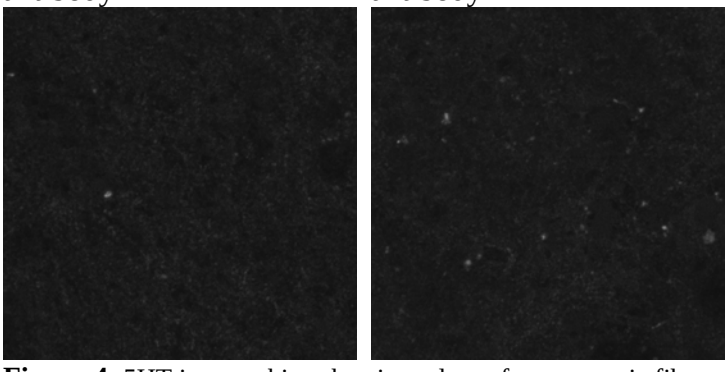

Figure 4. 5HT immunohistochemistry: loss of serotonergic fibers after spinal cord injury. ***A***, Immuno-labeling of 5HT, which labels serotonin containing fibers, in intact mouse. ***B***, Immuno-labeling of 5HT in SCI mouse. Serotonergic fibers are no longer present after SCI. ***C*** and ***D***, No primary antibody images for intact and SCI mice, respectively.

$5HT_{2C}$ receptors after spinal cord injury in quipazine and vehicle treated mice

To determine the number of $5HT_{2C}$ receptor clusters in intact and SCI mice, the method used is depicted in Fig. 5 below. First, the original images (Fig. 5A, B, C) were deconvolved in ImageJ. Deconvolving reduces the blurring artifact produced by the confocal microscope. A fluorescent bead is imaged with the confocal, and the rings around the bead are confocal-produced artifact. This reference bead image is used to reduce similar noise in immunohistochemical images from the confocal, and the result is dimmer background noise and sharper edges of fluorescently labeled objects (Hutcheon et al. 2000) (see Fig. 5D, E, F). The deconvolution algorithm used was downloaded as a macro from the ImageJ website (rsbweb.nih.gov/ij/). The algorithm uses the bead reference image to remove the blur that is known to be an artifact of the confocal imaging. The "Find Maxima" function on ImageJ was then used to detect points on the deconvolved image. This function is dependent on the noise tolerance, which can be manually changed and visualized. The noise tolerance was adjusted for the intact image so that all noticeable points were detected, and this tolerance value was then used for any SCI/saline and/or SCI/quipazine images from the same experiment, so that the images could be compared. The output type of Find Maxima was set to single points, and a binary image with one pixel for each maxima found was the output (5J, K, L). The macro "Grid of ROIs" (written by Dr. Nathan Cramer; ROI=region of interest) was then run on the binary image. This macro divided the image into 16 equally sized boxes, and counted the number of pixels (corresponding to the number of maxima) within each box. The final output on each image gave the pixel count for each box, so that there were 16 maxima values per image. This bin size allowed one image to be compared to another so

that a significant change in the number of maxima could be detected between intact and SCI conditions. A two-sided, unpaired t-test was used to compare the number of maxima between intact and SCI/saline, intact and SCI/quipazine, and SCI/saline and SCI/quipazine images. After p-values were obtained for each comparison in an experiment, the log of each p-value was taken, so that p-values could be averaged, as p values ranged from 0.02-5.26E-20. If multiple images were analyzed for one experiment, the logs of these p-values were averaged. Then, an overall average was taken, using one log of p-value per experiment, and this average was converted out of log form (10^average), giving an overall p-value for the change in number of receptors after SCI. The final result was an overall p value for the comparison of the number of maxima in intact vs. SCI/saline, intact vs. SCI/quipazine, and SCI/saline vs. SCI/quipazine. These p values are listed in Table 1, represented by (#). Significance for these three comparisons for each experiment is indicated in Fig. 6. It is important to note that only cords exposed to the exact same immunohistochemistry experiment and conditions were directly compared.

A. Intact, original **B**. SCI/saline, original **C**. SCI/quipazine, original

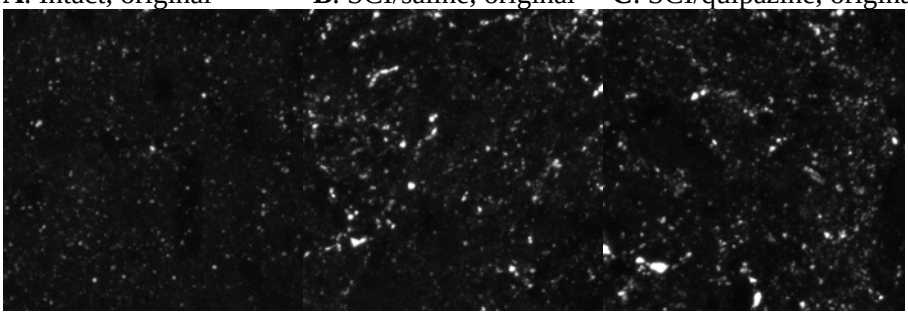

D. Intact, deconvolved **E**. SCI/saline, deconvolved **F**. SCI/quipazine, deconvolved

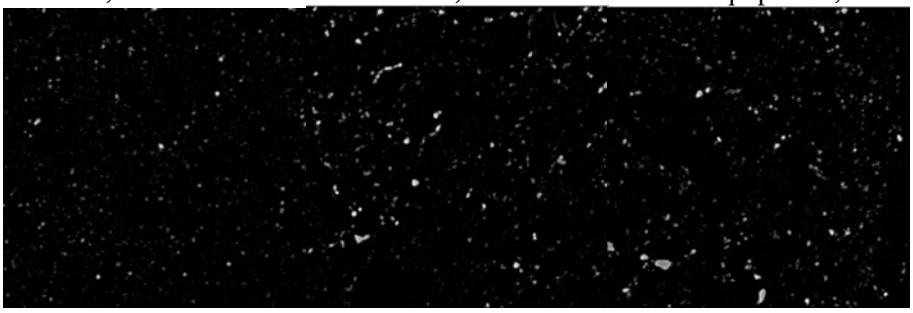

G. Intact, find maxima **H**. SCI/saline, find maxima **I**. SCI/quipazine, find maxima

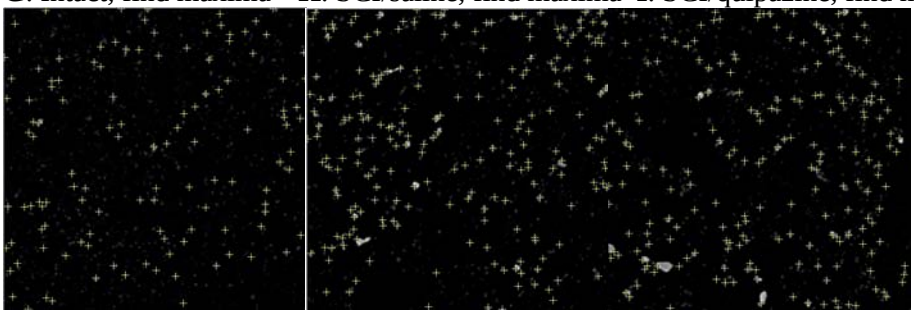

J. Intact, binary output 119 points **K**. SCI/saline, binary output 210 points **L**. SCI/quipazine, binary output 200 points

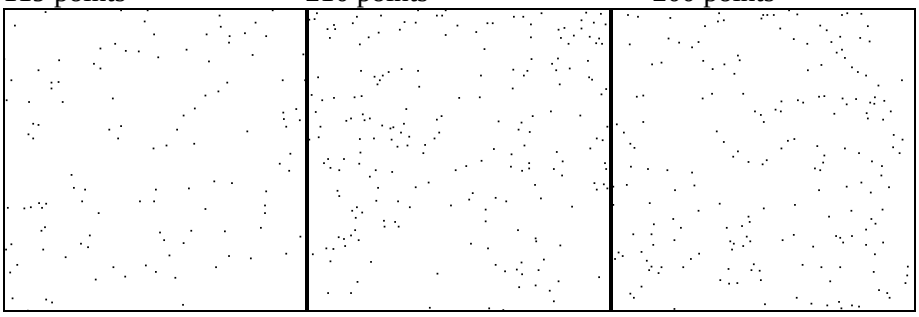

Figure 5. Finding maxima in ImageJ from intact (***A***, ***D***, ***G***), SCI/saline (***B***, ***E***, ***H***) and SCI/quipazine (***C***, ***F***, ***I***) mice. All images are 8 bit, 8-X zoom in medial lamina VIII (see Fig. 3), and are max projections of z-series. ***A***, ***B***, and ***C***, Original images from intact, SCI/saline, and SCI/quipazine mice, respectively. ***D***, ***E*** and ***F***, Deconvolved images of ***A***, ***B***, and ***C***, respectively. ***G***, ***H***, and ***I***, Corresponding images after a constant threshold is set for all images and the "Find Maxima" function in ImageJ is used. ***J***, ***K***, and ***L***, Binary outputs from the "Find Maxima" function.

Once an output for the total number of points in each image was generated for an experiment, all possible ratios comparing SCI/saline to intact, SCI/quipazine to intact, and SCI/saline to SCI/quipazine were calculated, depending on the mice surviving for each experiment. For the experiment shown in Fig. 5, the SCI/saline to intact ratio is 210 points/119 points, or 1.76; the SCI/quipazine to intact ratio is 200/119, or 1.68; and the SCI/saline to SCI/quipazine ratio is 210/200 or 1.05. Typically, there were two images per mouse per experiment; when this was the case, the two ratios were averaged to give a resultant average. For each experiment, there was one average ratio for SCI/saline to intact, SCI/quipazine to intact, and/or SCI/saline to SCI/quipazine. The ratios for each experiment are shown in Fig. 6. These three types of ratios were averaged for all experiments, and the results are summarized in Table 1.

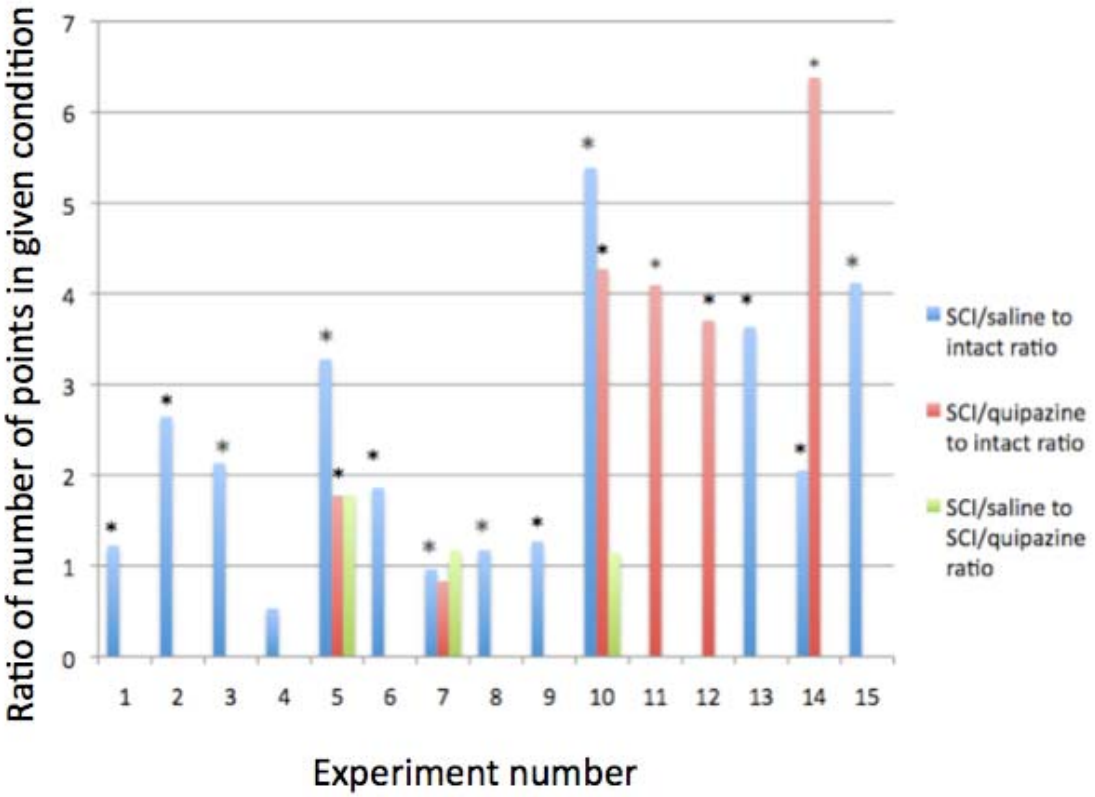

Figure 6. Ratios of number of points in $5HT_{2C}$ labeling for SCI/saline to intact, SCI/quipazine to intact, and SCI/saline to SCI/quipazine comparisons by experiment. * indicates $p < 0.05$ when number of points in $5HT_{2C}$ labeled images in an image were compared within an experiment. In comparing two images, significance was obtained by dividing each image into 16 boxes (Grid of ROIs macro) and having a point count for each box. Blue indicates SCI/saline to intact comparison, red indicates SCI/quipazine to intact comparison, and green indicates SCI/saline to SCI/quipazine comparison.

The SCI/saline to intact ratio across all experiments was significantly larger than 1 (Mean ± SD: 2.2 ± 1.5; n=13), as was the SCI/quipazine to intact ratio (2.9 ± 1.5; n=6). The SCI/saline to SCI/quipazine ratio across experiments was not significantly different that 1 (1.4 ± 0.4; n=3). These average ratios are shown in Table 1.

Table 1. Average ratios of number of points for three comparisons: SCI/saline to intact, SCI/quipazine to intact, and SCI/saline to SCI/quipazine.

	SCI/saline to intact comparisons	SCI/quipazine to intact comparisons	SCI/saline to SCI/quipazine comparisons
Mean of ratios of # points ± SD	2.2 ± 1.5*#; n=13	2.9 ± 1.5*#; n=6	1.4 ± 0.4; n=3

*=average ratio across all experiments significantly larger than 1.0 (p=0.003 for SCI/saline to intact; p=0.02 for SCI/quipazine to intact; p=0.16 for SCI/saline to SCI/quipazine; unpaired Student's t-test)

#=significant difference obtained by combining p values from within experiment image comparisons (by using Grid of ROIs macro described above) (p=0.007 for SCI/saline to intact; p=0.004 for SCI/quipazine to intact; p=0.153 for SCI/saline to SCI/quipazine; unpaired Student's t-test)

In addition to measuring the number of receptor clusters after SCI, a Matlab program developed by Adam McCann, a Master of Engineering student at Cornell University, was used to measure the pixel size and average intensity of each cluster or region of interest (ROI) (Fig. 7). First, the average intensity of the no primary antibody control image (Fig. 7B) was subtracted from the original image (Fig. 7A). Next, the subtracted images (Fig. 7C) were intensity thresholded, with the same threshold for all images to be compared (intact, SCI/saline, and/or SCI/quipazine) (Fig. 7D), and only pixels above this threshold are included in the next steps. Next, a morphological close operation is used to enforce the minimum blub radius of two pixels. Once the close operation is complete, a recursive region-growing algorithm is used to segment the ROIs and label each of the pixels in each ROI according to its assigned number. The resultant output is a mask structure that holds the ROI labels for the each of the pixels (Fig. 7E). Finally, the total number of pixels in each ROI as well as the total intensity value of each ROI is the calculated using the mask structure. Then, the total intensity of each ROI is divided by its area to obtain an "intensity density" value for each ROI.

A. $5HT_{2C}$ immunohisto-chemistry, original image

B. No primary antibody control

C. Image B after subtraction of no primary antibody

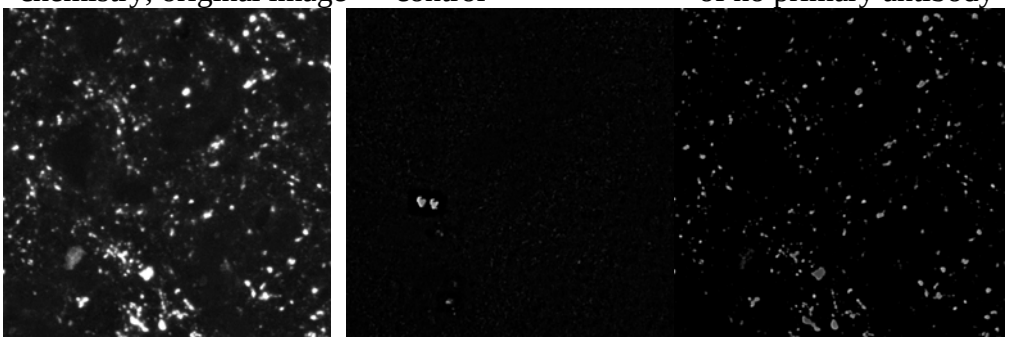

D. Binary output after setting intensity threshold

E. Mask for image C

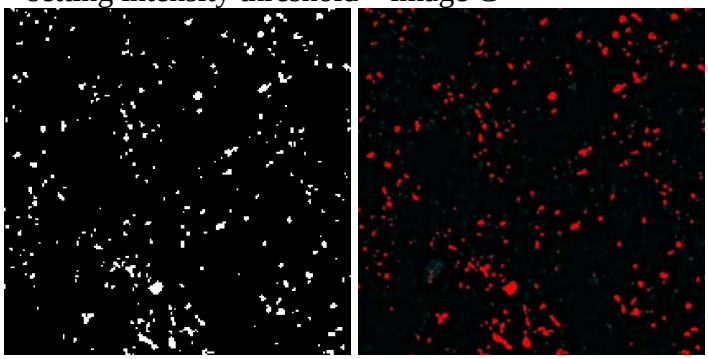

Figure 7. Matlab analysis to determine the size and intensity of $5HT_{2C}$ receptor clusters in intact, SCI/saline, and SCI/quipazine mice. First, the average intensity of the no primary antibody control (***B***) is subtracted from the original image (***A***), to adjust for tissue auto-fluorescence and non-specific binding of the secondary antibody. The resultant image (***C***) then has an intensity threshold applied in Matlab (***D***), and a minimum cluster radius is set for identifying regions of interest. The program uses a morphological close operation to remove regions under the cluster radius restriction, and then segments them to give a labeling mask structure for the deconvolved, no primary subtracted image (***E***).

A sample of the results from one experiment is shown in Fig. 8. Fig. 8A shows the area (in pixels) of each cluster found using the described Matlab program versus the cluster or ROI (region of interest) number assigned by the program for the intact mouse image. The maximum area for this image is 169 pixels, the mean area of the ROIs is 37 pixels, and 42 ROIs were found. Fig. 8B-C show ROI area results for an SCI/saline and an SCI/quipazine image from the same experiment, respectively. For the SCI/saline image (Fig. 8B), the maximum ROI area is 11683 pixels, the mean ROI area is 309 pixels, and 228 ROIs were found. For the SCI/quipazine image (Fig. 8C), the maximum

ROI area is 15968 pixels, the mean ROI area is 289 pixels, and 67 ROIs were found. In summary, for the example shown in Fig. 8A-B, the average area of the intact ROIs was smaller (37 pixels) than the average ROI areas for the SCI/saline (309 pixels) and SCI/quipazine (289 pixels) images. Additionally, the SCI/saline image had the most ROIs (228), while the intact had the least (42). After the average area of ROIs for each mouse was obtained, the average ROI areas for each experiment were compiled, and paired Student's t-tests were done to compare intact, SCI/saline, and SCI/quipazine average areas. The average areas and intensity densities from each experiment are shown in Fig. 9. For eight out of nine experiments, the average ROI area in SCI/saline mice was greater than that of intact mice of the same experiment, and the overall mean of ROI average areas across all experiments was significantly larger in SCI/saline (mean from all experiments=123 pixels; SD=84) as compared to intact; see Table 2 (mean from all experiments=65 pixels; SD=40) (n=9; p=0.046; Student's paired t-test). In comparing intact to SCI/quipazine, there was no significant difference in the mean area (intact mean=48 pixels, SD=31; SCI/quipazine mean=132 pixels, SD=101; n=5; p=0.13; paired Student's t-test). These results are summarized in Table 2. A paired t-test was done because of the variability between experiments; the same gain and laser power on the confocal was not used for each experiment, and the duration of the primary antibody incubation varied from 12-16 hours. Direct comparisons between experiments would be unreliable for these reasons.

A sample experimental output for the ROI "intensity density" is shown in Fig. 8D. There is much less variability between mice for these values; the mean intensity density of the ROIs is 226 for intact, 225 for SCI/saline, and 226 for SCI/quipazine. The

maximum ROI intensity density for intact was 231, 230 for SCI/saline, and 231 for SCI/quipazine. The means for all experiments were compiled in the same way the means for the areas were (see Fig. 9B for average intensity density values for each experiment). There were no significant differences between any groups across experiments.

A. Area of all ROIs within an intact image

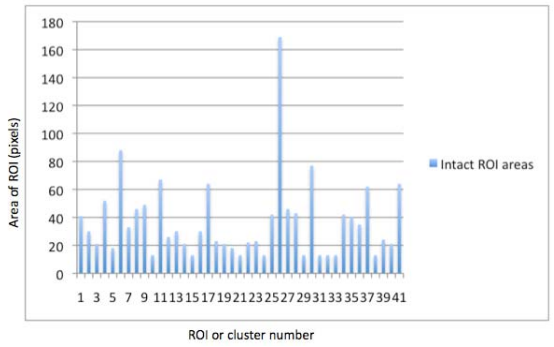

B. Area of all ROIs within an SCI/saline image

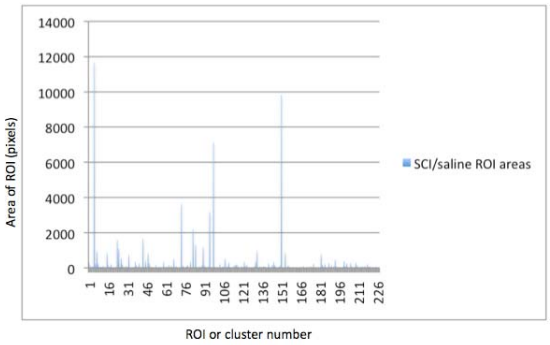

C. Area of all ROIs within an SCI/quipazine image

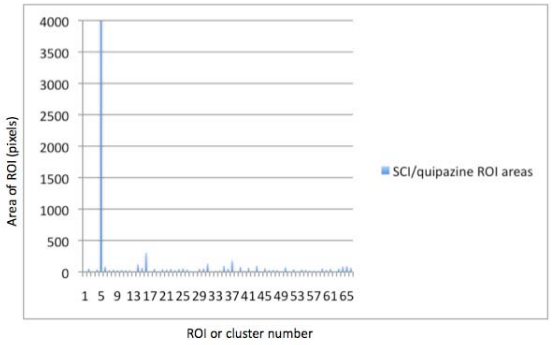

D. Intensity densities (intensity values per area) of all ROIs; intact, SCI/saline, and SCI/quipazine combined

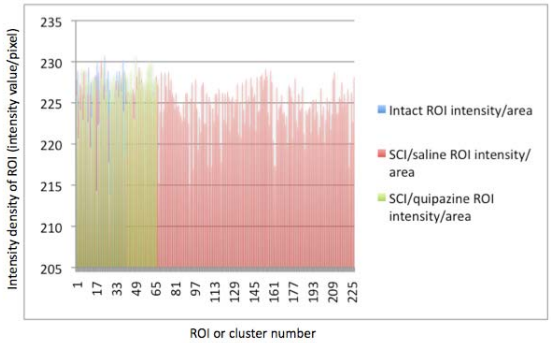

Figure 8. Area and intensity data from one experiment (intact, SCI/saline and SCI/quipazine). ***A-C***, Area (in pixels) of each ROI for intact, SCI/saline, and SCI/quipazine, respectively. The intact image has less ROIs than the SCI images, and the average area for intact is smaller than for SCI/saline or SCI/quipazine. The maximum ROI area for the intact image is less than 180 pixels (***A***), while most of the ROIs for SCI/saline and SCI/quipazine range from 0-2000 (***B***) and 0-500 (***C***), respectively. ***D***, Intensity density values for each ROI in intact, SCI/saline and SCI/quipazine from one experiment. These vales are closer to each other than the area values for intact, SCI/saline and SCI/quipazine. Blue represents intact mice, red represents SCI/saline mice, and green represents SCI/quipazine mice.

A summary of the results of the average $5HT_{2C}$ receptor cluster areas and intensity density values across all experiments is shown in Fig. 9 and Table 2.

A. Average area of clusters in intact, SCI/saline and SCI/quipazine mice, by experiment

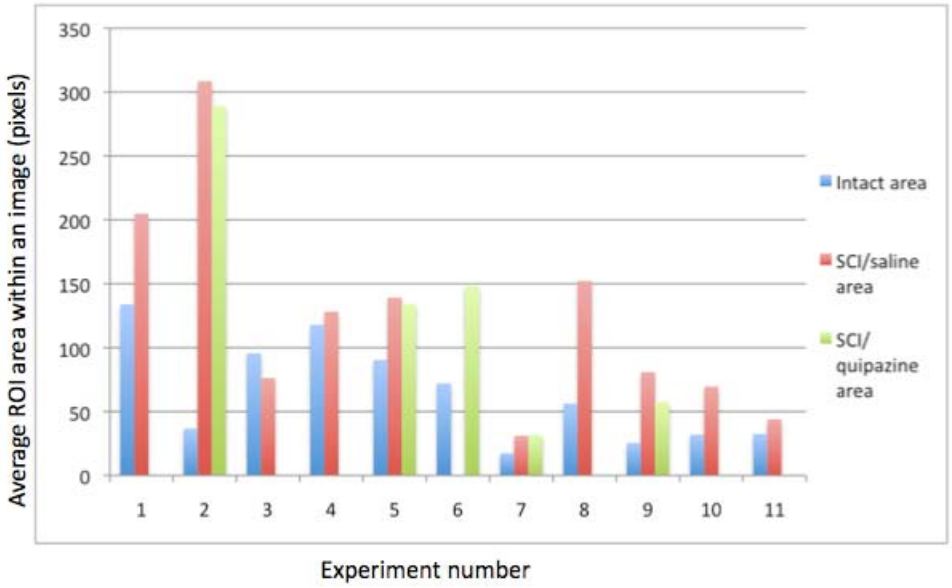

B. Average intensity density of clusters in intact, SCI/saline and SCI/quipazine mice, by experiment

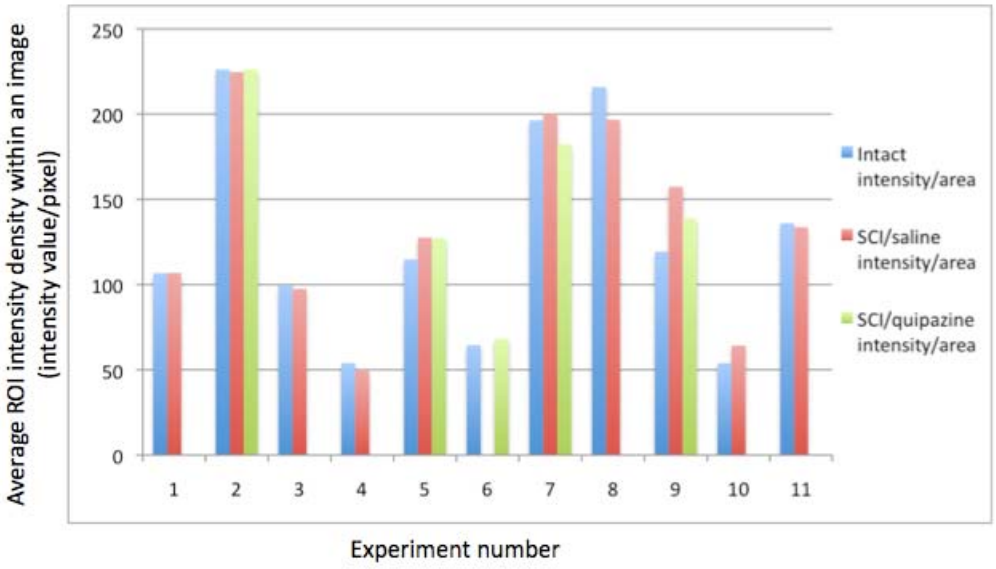

Figure 9. Summary of average area and intensity density of $5HT_{2C}$ receptor clusters by experiment. ***A***, Average pixel area of clusters (using the Matlab program described in the text) for each mouse in each experiment. ***B***, Average intensity density of clusters for each mouse in each experiment. Blue represents intact mice, red represents SCI/saline mice, and green represents SCI/quipazine mice.

Table 2. Summary of $5HT_{2C}$ cluster areas and intensity densities across experiments

	Intact (n=11)	SCI/saline (n=10)	SCI/quipazine (n=5)
Mean area of clusters ± SD	65 ± 40	123 ± 84*	132 ± 100
Mean intensity density of clusters ± SD	126 ± 62	136 ± 59	149 ± 60

*significantly different from intact (p=0.046, Student's t-test)

After spinal cord injury with no quipazine administration, $5HT_{2C}$ receptor clusters significantly increase in number and average area, but not average intensity density. There is no significant difference in the ratio SCI/saline # points to SCI/quipazine # points, indicating that daily quipazine administration does not have a significant effect on the number of $5HT_{2C}$ receptors after spinal cord injury.

Ca_V 1.3 channels after spinal cord injury in quipazine and vehicle treated mice

ImageJ was used to analyze Ca_V 1.3 images. Two types of measurements were obtained: a binary count of how many pixels were above a set threshold (Fig. 10I-J), and a measure of the mean intensity of the labeling that was above this threshold (Fig. 10K-L). Images were deconvolved as described for the $5HT_{2C}$ immuno-labeled images, and the average intensity of the deconvolved no primary antibody image was subtracted out (Fig. 10A-H). Then, ImageJ was used to automatically set a threshold for the intact image, and this same threshold was used for SCI images to be compared to intact. No SCI/quipazine images were analyzed, as there was only one experiment where the Ca_V 1.3 labeling was successful and an SCI/quipazine mouse was available. Once the threshold was set, a binary image was created, with black pixels above the threshold, and white pixels below the threshold (Fig. 10I-J). The percentage area of the image that was taken up by labeling could then be determined. Percentages for intact and SCI were compared; if there was

more than one image per intact or SCI mouse within an experiment, all percentages were averaged to give one mean percentage per mouse per experiment. A paired Student's t-test (n=4 experiments) was used to compare intact to SCI percentages across experiments, as percentage could vary between experiments are a result of different intensity settings on the confocal laser, different degrees of antibody washes during immunohistochemistry, and the exact length of time tissue was incubated in antibodies. However, these variables were kept exactly the same within an experiment, as SCI and intact tissues were directly adjacent on slides (see Fig. 1). A summary of the binary percentages for intact and SCI is shown in Table 3.

For the second component of the analysis, determining the average intensity of the pixels above threshold, the "Image Calculator" function in ImageJ was used to subtract the deconvolved, no primary subtracted image (8G-H) from the binary (resultant images: 8K-L). Histograms of the resultant images were done, and the mean intensities reported in Table 3. If more than one image was available per experiment for intact or SCI, the mean intensities were averaged for that mouse, so that only one mean intensity was given for each intact and SCI mouse within an experiment. As with the binary percentages, a paired Student's t-test (n=4 experiments) was done to compare the mean intact intensity to the mean SCI intensity across experiments.

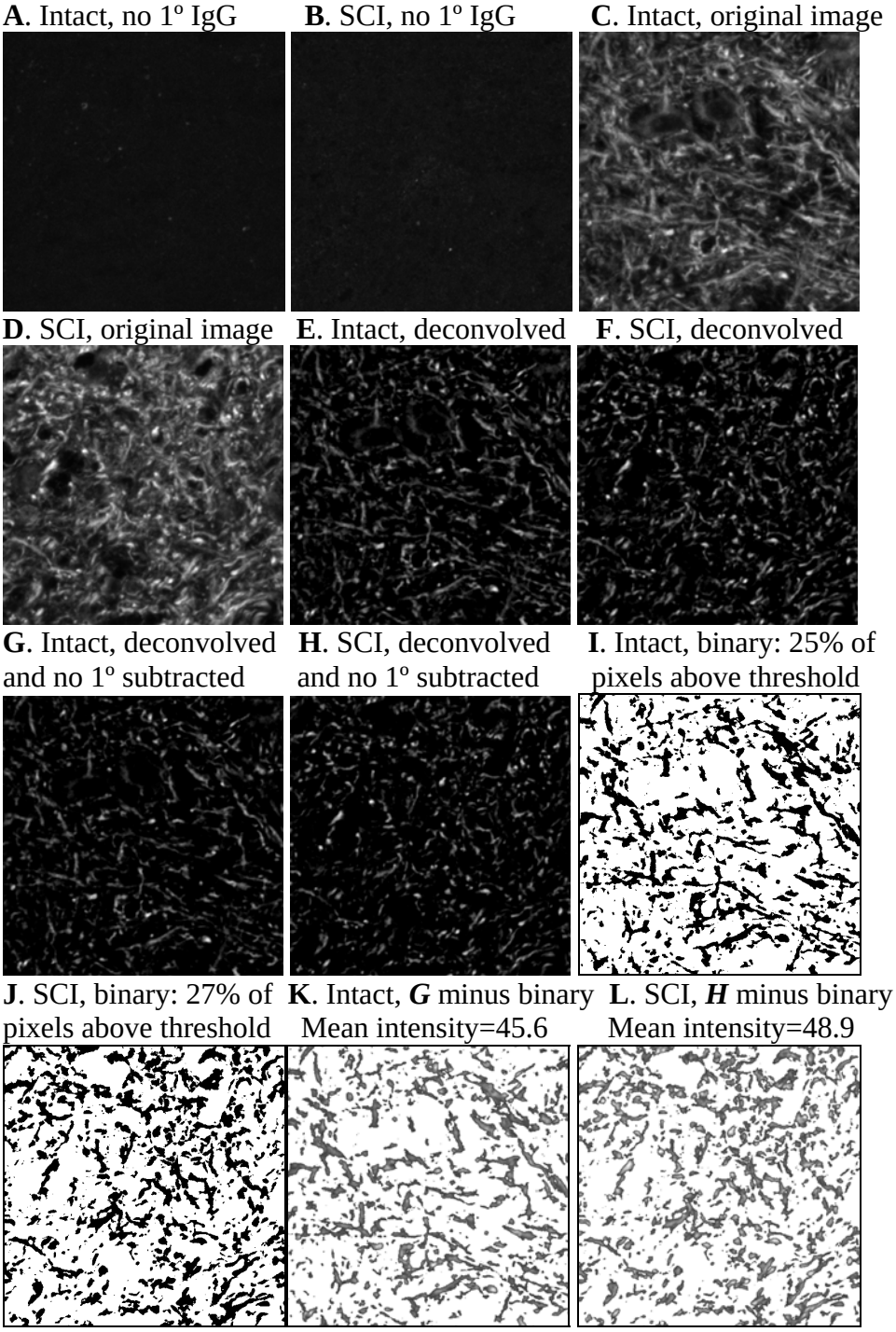

Figure 10. ImageJ analysis of Ca_V 1.3 images. ***A***-***B***, No primary antibody control images for intact and SCI, respectively. ***C***-***D***, Z-projections of z-series taken from the confocal in 1 µm steps (total ranges from 10-12 µm in a series) for intact and SCI, respectively. ***E***-***F***, Corresponding deconvolved images. ***G***-***H***, Corresponding results of subtracting the average intensity of the respective no primary images from the deconvolved images. ***I***-***J***, Binary outputs of ***G*** and ***H***, with the same intensity threshold set for both. Here, 24.7% of the pixels are above threshold for intact, and 27.3% of the pixels are above threshold for SCI. ***K***-***L***, Result of subtracting the images in ***G*** and ***H*** (using the "Image Calculator" in ImageJ) from their respective binary images, giving the intensity values of all pixels above threshold. The mean intensity was 45.6 for intact and 48.9 for SCI here.

Table 3. Summary of $Ca_V1.3$ analysis results.

	Percentage of pixels above threshold (n=4 mice, 8 images)	Mean intensity value of pixels above threshold
Intact, mean ± standard deviation	21.8 ± 0.09	46.5 ± 24.0
SCI, mean ± standard deviation	36.4 ± 0.15	72.6 ± 39.9
p value (paired Student's t-test)	0.028	0.047

The results of the $Ca_V1.3$ analysis are shown in Table 3. In the binary images, there was a significantly higher percentage of pixels above threshold in the SCI condition (36.4 ± 0.15) as compared to intact (21.8 ± 0.09) (n=4; paired Student's t-test; p=0.028). When the binary images were subtracted from the original images, the mean intensity was significantly higher in the SCI (72.6 ± 39.9) images as compared to intact (46.5 ± 24.0) (n=4; paired Student's t-test; p=0.047). All images used were 16-bit, and intensity values range from 0 (black) to 4095 (white, saturation).

Distribution of the serotonin transporter after spinal cord injury in quipazine and vehicle treated mice

As there was only an n of two experiments, no analysis was done on the serotonin transporter immunohistochemistry. One result is shown in Fig. 11, along with the no primary antibody controls.

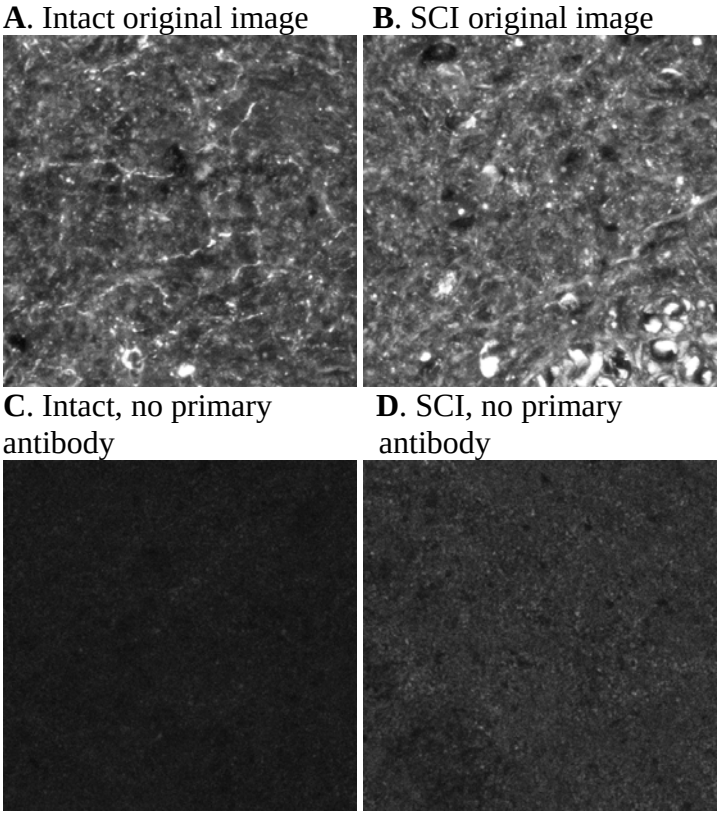

Figure 11. Example of serotonin transporter (SERT) labeling (unaltered images), taken from medial lamina VIII of spinal cord (Fig. 3). Images are z-projections of z-series, as in Fig. 5A-B, with 10-12 µm of tissue imaged in 1 µm steps. ***A***, intact mouse. ***B***, SCI/saline mouse. ***C***-***D***, No primary antibody controls for intact and SCI/saline, respectively. All four images were obtained with the exact same confocal settings.

Discussion

After spinal cord injury, there is a significant upregulation in the number of $5HT_{2C}$ receptor clusters, both with and without quipazine administration. The average area of these receptor clusters is larger after SCI, significantly larger for SCI/saline but not significant for SCI/quipazine.

Because spinal cord injury cuts off the descending serotonergic input from the Raphe nuclei, neurons caudal to the lesion site no longer receive serotonergic input. A loss of 5HT would be expected to cause homeostatic changes to adjust to this loss. For example, neurons with 5HT receptors may increase receptor expression in order to become activated by a smaller amount of 5HT. Intact mice have $5HT_{2C}$ receptors

throughout the gray matter of the upper lumbar spinal cord, and in the ventral half of the cord, these receptors are post-synaptic (not autoreceptors) (Schmidt and Jordan 2000). Because $5HT_{2C}$ receptors have post-synaptic functions in the medial lamina VIII region of the upper lumbar spinal cord, we would expect there to be a homeostatic upregulation in the expression levels after SCI. Using ImageJ, there was a significant increase in the number of $5HT_{2C}$ receptors. This increase in the number of receptors may represent new sites of $5HT_{2C}$ on dendrites. Additionally, we found that the average area of $5HT_{2C}$ receptor clusters after SCI (no quipazine) was significantly larger than the average area of receptor clusters in intact mice within each experiment. This increase in the area of receptor clusters after SCI could mean that at each receptor cluster, there is an increased expression of $5HT_{2C}$ receptors. The average brightness of the clusters is not significantly different after SCI, and does not appear to trend towards any difference between groups. An increase in brightness could translate to a higher concentration of receptors at a given area, which we did not observe. Together, the area and intensity results suggest that after SCI, each cluster of $5HT_{2C}$ receptors covers more area, but each cluster does not increase in density of $5HT_{2C}$ expression. One possible explanation for this expression pattern is that in intact mice, there is already a maximal or optimal concentration of $5HT_{2C}$ expression at each cluster, and there is simply not enough room on the membrane to increase the density of $5HT_{2C}$ expression after SCI.

Because there are more, larger, $5HT_{2C}$ receptor clusters in spinal cord injured mice, as compared to intact mice, it may be expected for neurons with $5HT_{2C}$ receptors to be more sensitive to 5HT after SCI. Electrophysiological experiments by Dr. Andreas Husch from our lab have shown that V2a interneurons, which are hypothesized to play a

role in the locomotor CPG and are located in the intermediate zone of the spinal cord, in intact mice are unresponsive to 0.1 µm 5HT, show weak excitation in 1 µm 5HT (firing frequency less than 1 Hz in the recording in Fig. 12), and the strongest excitation with 10 µm 5HT (up to 2 Hz in the recording in Fig. 12). However, recordings from V2a interneurons from mice sacrificed four weeks after SCI surgery are strongly responsive to 0.1 µm 5HT and higher, with firing frequency reaching 8 Hertz (Fig. 12) The same SCI surgery protocol is used for these mice as the protocol described in the Methods section above.

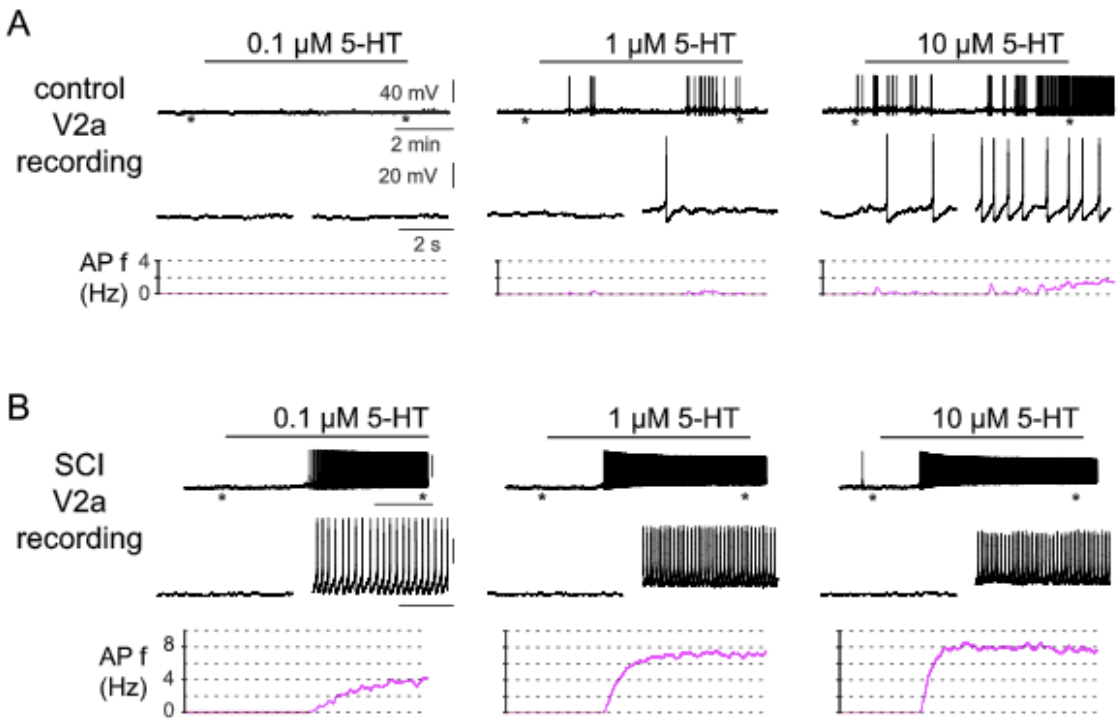

Figure 12. "**In SCI mice, V2a interneurons are 5HT supersensitive.** A) Perforated Patch recording of a silent control V2a interneuron. Application of 0.1 µM 5HT did not change the activity of the interneuron. While application of 1 µM 5HT shows weak effects on activity, 10 µM 5 HT applications depolarizes the membrane potential and elicits 1-2 Hz firing (right). B) Perforated Patch recording of a silent SCI V2a interneuron. Application of 0.1 µM 5 HT depolarized the membrane potential and initiated tonic firing up to 4 Hz. (left) Application of 1 or 10 µM 5 HT lead to depolarization and AP firing at higher frequencies. The asterisks indicate the times of expanded views of the firing activity." (Husch, unpublished data)

We hypothesized that daily administration of quipazine, a $5HT_2$ agonist, may act as partial 5HT replacement therapy and reduce the upregulation of $5HT_{2C}$ receptor clusters after SCI. However, we did not observe a reduction in upregulation of $5HT_{2C}$ in SCI/quipazine mice as compared to SCI/saline mice; in fact, the mean ratios of the number of clusters in SCI/quipazine as compared to intact mice (2.6 ± 1.5) was slightly (though not significantly) larger than the ratio for SCI/saline to intact (2.2 ± 1.5) (Table 1). Because there was still a significant upregulation of $5HT_{2C}$ receptor clusters in SCI mice receiving daily quipazine administration, quipazine alone is insufficient to reduce $5HT_{2C}$ upregulation. Additionally, electrophysiological experiments from our lab have shown that V2a interneurons from SCI/quipazine mice show the same sensitivity to 5HT as SCI/saline mice do, responding with a high firing frequency and depolarization with 0.1 μm 5HT (Husch, unpublished data). One reason for this maintained $5HT_{2C}$ upregulation and 5HT hypersensitivity may be the nature of the administration, as mice receive quipazine once daily as an intraperitoneal injection. Thus, the concentration of quipazine in the spinal cord is likely not constant throughout the day, and its application does not mimic natural conditions, where 5HT levels rise and fall over the course of a day (Reiter 1976). To address this concern, a similar immunohistochemistry experiment could be done on SCI mice that receive quipazine via an implanted osmotic mini-pump that administers a fixed concentration directly to the spinal cord (Antri et al. 2003). Quipazine alone would not likely be used to treat humans with spinal cord injuries. It does not mimic the natural levels of 5HT in the spinal cord; to accurately regulate levels, administration would have to be timed precisely and likely occur fairly frequently. Additionally, quipazine is a $5HT_2$ agonist; there are other 5HT receptor subtypes in the

spinal cord that are involved in locomotion (Landry et al. 2006; Madriaga et al. 2004; Schmidt and Jordan 2000), and binding $5HT_2$ alone does not reduce 5HT sensitivity. As there was a significant upregulation of $5HT_{2C}$ receptors in four out of five SCI/quipazine mice, another shortfall of quipazine is that it is not activating the homeostatic pathway that prevents $5HT_{2C}$ upregulation after SCI, demonstrating its inability to mimic all of the actions of 5HT. Because quipazine did not reduce the upregulation of $5HT_{2C}$ after SCI, and V2a interneurons from SCI/quipazine mice are sensitive to 0.1 µm 5HT, these neurons are still hypersensitive to 5HT. Quipazine alone does not seem to mediate homeostatic changes in $5HT_{2C}$ receptor expression that occur after spinal cord injury.

Another result of spinal cord injury is a significant increase in the area and the intensity of the medial lamina VIII region covered by Ca_V 1.3 voltage-gated calcium channels (Table 3). An increase in the total area covered by Ca_V 1.3 channels could be the result of an increase in Ca_V 1.3 expression levels at more places on the dendrites, while an increase in the intensity could mean a higher density of Ca_V 1.3 channels at each site where the channels are found. Ca_V 1.3 channels are L-type channels, meaning that they facilitate a slow, but long-lasting inward current (Li et al. 2007; Bell et al. 2001). In normal neurons, Ca_V 1.3 channels mediate a voltage-dependent persistent inward calcium current that is activated by 5HT (Li et al. 2007). As Ca_V 1.3 channels respond to 5HT, and there is a 5HT loss following SCI, our hypothesis of homeostatic compensation would predict that Ca_V 1.3 expression levels would increase to compensate for 5HT loss. Together, the increase in area and intensity of Ca_V 1.3 channels following SCI point to an overall increase in the expression level of Ca_V 1.3 channels, another consequence of SCI that could contribute to V2a interneuron hypersensitivity to 5HT.

One consequence of spinal cord injury that impacts the quality of life for humans is involuntary leg muscle spasms. There are multiple changes at the neural and molecular levels that occur following SCI related to 5HT loss that could possibly contribute to this muscle spasticity. In addition to the hypersensitivity to 5HT in interneurons observed in our lab, Murray et al. (2011) found there to be an increase in the number of constitutively active $5HT_{2C}$ receptors in rat motoneurons after SCI, meaning these motoneurons can become activated in the absence of 5HT. Thus, after SCI, neurons involved in producing locomotor output can respond to a lower than normal physiological concentration of 5HT or activate in the absence of 5HT (when they normally require 5HT to become activated). This general hyperactivity can partially explain why involuntary muscle spasms in SCI patients occur, and suggests routine administration of the right combination of 5HT agonists may help to reduce homeostatic changes that lead to 5HT sensitivity. Indeed, Guertin (2009) found that when SCI mice were regularly administered a cocktail of dopaminergic and serotonergic receptor subtype agonists, mice exhibited locomotor recovery and were able to take weight-bearing steps with plantar foot placement. Work is currently being done in the field to obtain an optimal treatment cocktail.

Our lab is currently exploring the effects of SCI on the distribution of the serotonin transporter (SERT). Its homeostatic changes after SCI may also contribute to 5HT sensitivity in V2a interneurons as well as other serotonergic neurons. In intact mice, SERT, located along synaptic boutons of serotonergic fibers, removes 5HT from the synaptic cleft following synaptic transmission. After SCI, serotonergic fibers from the hindbrain degenerate along with SERT; thus, when neurons in the upper lumbar region are exposed to endogenous 5HT, there are fewer 5HT transporters to remove the 5HT

from the surrounding synaptic cleft. The increased firing frequency of SCI neurons shown in Fig. 12 could partially be explained by this loss of SERT; the effective dose of 5HT would be larger for neurons from SCI mice as compared to intact mice because of the loss of SERT. If SERT loss is a contributing factor to 5HT sensitivity, then it should be possible for 5HT sensitivity to exist without an increase in the number of 5HT receptors. Our lab is currently exploring this hypothesis by applying citalopram, a SERT blocker, to V2a interneurons from intact mice and using perforated patch recordings to measure neural responses to 5HT (Husch, unpublished data). Blocking the 5HT transporters increases sensitivity to 5HT, indicating that a loss of SERT after SCI contributes to 5HT sensitivity. A future goal is to continue SERT immunohistochemistry experiments, like that shown in Fig. 11, to determine whether there is a loss of SERT after SCI. We also intend to analyze the $5HT_{2C}$ images in 3D to compare volume and intensity densities of receptor clusters, to further understand the changes in receptor clusters following spinal cord injury.

Conclusions

The network of neurons that generates the rhythmic alternation of legs (in humans) and fore- and hindlimbs (in other animals) to produce walking is complex and not fully understood. A variety of neuromodulators play various roles in the activation of different neuron types, creating a complex circuit of excitation and inhibition. The CPG is not completely rigid, however; it must also have flexibility, as animals walk at different speeds and sensory feedback can influence locomotor output. It would follow that spinal cord injuries that occur anterior to this CPG disrupt normal communication between the brain as well as peripheral nerves anterior to the injury site. We cannot predict the

entirety of the effects SCI can have on the CPG, and thus cannot yet hope to reverse all of the effects of SCI once it occurs. However, we can elucidate specific components of the effects, and eventually put together a more complete picture. Here, we found that after SCI, the number and average size of $5HT_{2C}$ receptor clusters increases, as well as the area and mean intensity of Ca_V 1.3 channels. Hayashi et al. (2010) found that SERT is down-regulated after severe spinal cord contusions, and Murray et al. (2011) found that there are more constitutively active $5HT_{2C}$ receptors after. Likely, many more receptor subtypes and channels are affected in different ways by SCI, and only by using multiple approaches such as immunohistochemistry and electrophysiology can we hope to elucidate all the effects of spinal cord injury, and how we can mediate those effects to increase quality of life.

Footnotes

This work was supported by National Institutes of Health Grant NS057599. I would like to thank Dr. Cramer for establishing protocols, Sylvia Allen and Connor Benton for mouse husbandry, Carol Bayles for help with confocal imaging, and Adam McCann for work in Matlab. I would also like to thank everyone in the Harris-Warrick lab for their insights along the way.

References

Antri M, Mouffle C, Orsal D, Barthe JY. 2003. 5-HT_{1A} receptors are involved in short and long-term processes responsible for 5-HT-induced locomotor function recovery in chronic spinal rat. *Eur J Neurosci*. 18(7):1963-72.

Ballion B, Branchereau P, Chapron J, Viala D. 2002. Ontogeny of descending serotonergic innervation and evidence for intraspinal 5-HT neurons in the mouse spinal cord. *Brain Res Dev Brain Res*. 137(1):81-8.

Bell DC, Butcher AJ, Berrow NS, Page KM, Brust PF, Nesterova A, Stauderman KA, Seabrook GR, Nurnberg B, Dolphin AC. 2001. Biophysical properties, pharmacology, and modulation of human, neuronal L-type ($alpha_{1D}$, Ca_V 1.3) voltage-dependent calcium currents. *J Neurophysiol*. 85(2):816-27.

Cormier CM, Mukhida K, Walker G, Marsh DR. 2010. Development of autonomic dysreflexia after spinal cord injury is associated with a lack of serotonergic axons in the intermediolateral cell column. *J Neurotrauma*. 27(10):1805-18.

Guertin PA. 2009. Recovery of locomotor function with combinatory drug treatments designed to synergistically activate specific neuronal networks. *Curr Med Chem*. 16(11):1366-71.

Harris-Warrick RM. 2010. General principles of rhythmogenesis in central pattern generator networks. *Prog Brain Res*. 187:213-22.

Hayashi Y, Jacob-Vadakot S, Dugan EA, McBride S, Olexa R, Simansky K, Murray M, Shumsky JS. 2010. 5-HT precursor loading, but not 5-HT receptor agonists, increases motor function after spinal cord contusion in adult rats. *Exp Neurol*. 221(1):68-78.

Hutcheon B, Brown LA, Poulter MO. 2000. Digital analysis of light microscope immunofluorescence: high-resolution co-localization of synaptic proteins in cultured neurons. *J Neurosci Methods*. 96(1):1-9.

Jackson DA, White SR. 1990. Receptor subtypes mediating facilitation by serotonin of excitability of spinal motoneurons. *Neuropharmacology*. 29(9):787-97.

Jordan LM, Liu J, Hedlund PB, Akay T, Pearson KG. 2008. Descending command systems for the initiation of locomotion in mammals. *Brain Res Rev*. 57(1):183 91.

Kiehn O. 2006. Locomotor circuits in the mammalian spinal cord. *Annu Rev Neurosci*. 29:279-306.

Landry ES, Lapointe NP, Rouillard C, Levesque D, Hedlund PB, Guertin PA. 2006. Contribution of spinal 5-HT_{1A} and 5-HT_7 receptors to locomotor-like movement induced by 8-OH-DPAT in spinal cord-transected mice. *Eur J Neurosci*. 24(2):535-46.

Li X, Murray K, Harvey PJ, Ballou WE, Bennett DJ. 2007. Serotonin facilitates a persistent calcium current in motoneurons of rats with and without chronic spinal

cord injury. *J Neurophysiol*. 97(2):1236-1246.

Madriaga MA, McPhee LC, Chersa T, Christie KJ, Whelan PJ. 2004. Modulation of locomotor activity by multiple 5-HT and dopaminergic receptor subtypes in the neonatal mouse spinal cord. *J Neurophysiol*. 92(3):1566-76.

McCall RB, Aghajanian GK. 1979. Serotonergic facilitation of facial motoneuron excitation. *Brain Res*. 169:11-27.

Murray KC, Stephens MJ, Ballou EW, Heckman CJ, Bennett DJ. 2011. Motoneuron excitability and muscle spasms are regulated by $5HT_{2B}$ and $5HT_{2C}$ receptor activity. *J Neurophysiol*. 105(2):731-48.

Reiter RJ. 1976. Pineal and associated neuroendocrine rhythms. *Psychoneuroendocrinology*. 1(3):255-63.

Schmidt BJ, Jordan LM. 2000. The role of serotonin in reflex modulation and locomotor rhythm production in the mammalian spinal cord. *Brain Res Bull*. 53(5):689-710.

VanderMaelen CP, Aghajanian GK. 1980. Intracellular studies showing modulation of facial motoneurone excitability by serotonin. *Nature*. 287(5780):346-7.

White SR, Neuman RS. 1983. Pharmacological antagonism of facilitatory but not inhibitory effects of serotonin and norepinephrine on excitability of spinal motoneurons. *Neuropharmacology*. 22(4):489-94.

Zhong G, Droho S, Crone SA, Dietz S, Kwan AC, Webb AC, Sharma K, Harris-Warrick RM. 2010. Electrophysiological characterization of V2a interneurons and their locomotor-related activity in the neonatal mouse spinal cord. *J Neurosci*. 30(1):170-82.